

Articles

Synthesis and Characterization of Thermoresponsive-*co*-Biodegradable Linear–Dendritic Copolymers

Young Shin Kim,^{‡,‡} Eun Seok Gil,[†] and Tao Lu Lowe^{†,‡,§,*}

Departments of Surgery, Bioengineering, and Materials Science and Engineering, The Pennsylvania State University, 500 University Drive, Hershey, Pennsylvania 17033

Received February 5, 2006; Revised Manuscript Received September 6, 2006

ABSTRACT: A novel linear–dendritic copolymer containing thermoresponsive poly(*N*-isopropylacrylamide) (PNIPAAm), hydrophobic and biodegradable poly(L-lactic acid) (PLLA), and hydrophilic poly(L-lysine) (PLL) dendrons was designed, synthesized and characterized. The thermoresponsive-*co*-biodegradable linear–dendritic copolymer was synthesized by 1,3-dicyclohexylcarbodiimide (DCC) coupling reaction of three generation PLL dendron and PNIPAAm grafted with PLLA. UV–vis spectroscopy and dynamic light scattering measurements demonstrated that the linear–dendritic copolymer was thermoresponsive by showing a lower critical solution temperature whose value depended on the linear–dendritic copolymer concentrations. The viscosity and molar mass of the linear–dendritic copolymer decreased with time in PBS (pH = 7.4) solutions indicating that the linear–dendritic copolymer is degradable. FTIR measurements further revealed that the degradation of the linear–dendritic copolymer was due to the hydrolytic degradation of the ester bonds of the PLLA component.

Introduction

Dendrimers, nanoscale highly branched and reactive three-dimensional macromolecules, become increasingly important in biomedical applications due to their specific size, intriguing structural properties such as internal voids and cavities, and a highly functional terminal surface.^{1–3} Particularly, the spatially arranged functional groups can be used for postformation modifications on the periphery of the dendritic globules⁴ with a variety of molecules such as small molecule drugs,⁵ DNA^{6–10} and oligonucleotides^{11,12} for drug delivery and gene therapy, targeting molecules such as folic acid to localize drugs to desired tissue sites,^{8,13–16} hydrophilic molecules such as PEO to increase their blood circulation times,^{5,17,18} and contrast agents to use in magnetic resonance imaging (MRI).^{17–21} More uniquely, the functional groups of the dendrimers can incorporate two and more functional molecules mentioned above for more compact and efficient therapeutic treatments and diagnostics. Furthermore, when dendrimers are conjugated on the both ends of linear polymers becoming linear–dendritic copolymers, they have great potency in increasing drug payload due to their supramolecular micelles structures.^{22–26} Despite these advantages, the currently available dendrimers or linear–dendritic copolymers cannot achieve long-term drug release at the same time in response to environmental changes (such as temperature, pH, etc.), which is in need for the treatment of many chronic

diseases. In this work, we have developed a novel strategy to introduce both thermoresponsive and biodegradable properties into linear–dendritic copolymer for the purpose of targeted and sustained drug delivery in response to chemical, physical, and biological stimuli.^{27,28}

The thermoresponsive-*co*-biodegradable linear–dendritic copolymer that we have developed contains thermoresponsive poly(*N*-isopropylacrylamide) (PNIPAAm), hydrophobic and biodegradable poly(L-lactic acid) (PLLA), and hydrophilic cationic poly(L-lysine) (PLL) dendrons. The PNIPAAm is chosen as a thermoresponsive moiety due to its unique phase transition at a lower critical solution temperature (LCST) in the vicinity of 32 °C. It expands and swells when cooled below its LCST, and it shrinks and collapses when heated above its LCST. When PNIPAAm is incorporated with hydrophobic and hydrophilic units, the PNIPAAm-based polymers have been shown to have the following advantages in drug delivery: (1) by allowing aqueous loading of hydrophilic therapeutic agents at temperatures lower than the LCSTs with high loading efficiency avoiding the use of organic solvents that result in denaturation of therapeutic proteins;²⁹ (2) by modulating the mechanism of the biodegradation of biodegradable polymers;^{28,30,31} (3) by decreasing the cytotoxicity of polycationic polymers;³² (4) by thermally localizing drugs to targeted sites after systemic injections when their LCSTs are tailored to the temperatures between 37 (body temperature) and 42 °C (used routinely in clinical hyperthermia);^{33–35} (5) by releasing therapeutic agents at different profiles in response to temperature, pH and other stimuli.^{36–38} The rationale behind the choice of PLLA is due to its combination of hydrophobicity and biodegradability,^{39–41} which can modify (decrease) the LCST of the PNIPAAm and achieve sustained release of therapeutic agents. PLL dendron is chosen because of its peptide and hydrophilic natures and

* Corresponding author: E-mail: tlowe@psu.edu. Telephone: 717-531-8602. Fax: 717-531-4464.

[†] Department of Surgery.

[‡] Department of Bioengineering.

[§] Department of Materials Science and Engineering.

[‡] Current address: University of Delaware, Materials Science and Engineering, 201 Dupont Hall, Newark, DE 19716. E-mail: youngkim@udel.edu.

great amount of terminal free amine groups. The hydrophilic nature of the PLL can modify (increase) the LCST of the PNIPAAm. The polyamine groups of the PLL can enhance delivery of therapeutic agents into cells or across biological barriers due to their electrostatic interaction with the polyanionic phospholipids of cell membranes and bulky branched structure.^{9,42,43}

In this work, we designed and synthesized the thermoresponsive-co-biodegradable linear-dendritic copolymer. We characterized the chemical structure of the linear-dendritic copolymer by using ¹H nuclear magnetic resonance (NMR) technique. We measured the size of the linear-dendritic copolymer in dry and wet states by using TEM and dynamic light scattering, respectively. We studied the thermoresponsive properties of the linear-dendritic copolymer using UV-vis spectroscopy and dynamic light scattering (DLS). We investigated the hydrolytically degradable properties of the linear-dendritic copolymer at temperatures below and above the LCST by viscometer, matrix assisted laser desorption/ionization time-of-flight (MALDI-TOF) and Fourier transform infrared spectroscopy (FTIR) techniques.

Experimental Section

Materials. Poly(L-lactic acid) (PLLA, $M_w = 2000 \text{ g}\cdot\text{mol}^{-1}$ and $M_n = 1835 \text{ g}\cdot\text{mol}^{-1}$) was purchased from Polysciences, Inc. Warrington, PA. The following materials were obtained from Sigma-Aldrich, Inc., St. Louis, MO: *N*-isopropylacrylamide, 1,3-dicyclohexylcarbodiimide (DCC), allylamine, *N*-hydroxybenzotriazole (HOBT), 2,5-dihydroxybenzoic acid, *N,N*-dimethylformamide (DMF, HPLC grade), methylene chloride (CH_2Cl_2 , HPLC grade), ether, methanol, 2-aminoethanethiol, pentanedione peroxide, trifluoroacetic acid (TFA), triisopropylsilane (TIS), piperidine, deuterated chloroform (CDCl_3), and tetrahydrofuran (THF). *N*- α -(9-Fluorenylmethoxycarbonyl)- ϵ -Lys₄-Lys₂-Lys- β Ala-Wang resin (Fmoc₈-Lys₄-Lys₂-Lys- β Ala-Wang resin) was purchased from Calbiochem, San Diego, CA. All the chemicals were used as received. Deionized distilled water was used in all the experiments. Dialysis membrane (MWCO 3500 Da) and a glass filter frit were purchased from Spectrum Laboratories, Rancho Dominguez, CA and Chem-glass, Vineland, NJ, respectively.

Synthesis of Linear-Dendritic Copolymer. PLLA terminated with allyl groups was synthesized by DCC coupling reaction of PLLA and allylamine. PLLA (1 mmol, 2 g) was dissolved in the mixture solvent of DMF and CH_2Cl_2 (3:7 v/v) at room temperature. DCC (1.3 mmol, 0.268 g) and HOBT (1.3 mmol, 0.175 g) were predissolved in a small amount of the mixture solvent, respectively, and then added into the PLLA solution in the presence of nitrogen. After 1 h, allylamine (1.3 mmol, 0.0975 g) was added dropwise with moderate stirring, and the reaction proceeded at room temperature for 5 h. After dicyclohexylurea (DCU) side product was removed by filtration, final solution was precipitated in ether and dried in a vacuum for 1 day. The resulting product was washed twice with methanol to remove unbound allylamine, DCC, and HOBT, filtered and dried in a vacuum for 1 day. The yield of this reaction was 90%.

PNIPAAm grafted with PLLA was synthesized by free radical polymerization. Monomer NIPAAm (20 mmol, 2.263 g, Aldrich), macromer PLLA terminated with allyl groups (0.02 mmol, 0.041 g), transfer agent 2-aminoethanethiol (1 mmol, 0.113 g), and initiator pentanedione peroxide (0.3 mol % of total monomers) were dissolved in DMF (5 mL). The solution was degassed by freezing and thawing method. The reaction was conducted under nitrogen condition at 100 °C for 4 h. The solution was precipitated with 10-fold excess ether and filtered and dried in a vacuum for 1 day. To remove unbound chemical compounds including 2-aminoethanethiol, pentanedione peroxide, NIPAAm monomer and PLLA terminated with allyl groups, the polymer solution was dialyzed against DMF for 6 h. For further purification, the polymers were

dissolved in water at 50 $\text{mg}\cdot\text{mL}^{-1}$ and centrifuged to precipitate unbound PLLA at 3000 rpm at 25 °C for 1 h. The supernatant was carefully taken out and centrifuged at 31 °C for 1 h to remove PNIPAAm homopolymer, which has a LCST of 32 °C. These processes were done three times. The precipitated PNIPAAm grafted with PLLA was dissolved in water and lyophilized. The yield of this reaction was 82%. Homogeneous PNIPAAm was synthesized under the same condition for comparison.

Fmoc₈-Lys₄-Lys₂-Lys- β Ala terminated with carboxylic acid was obtained by cleaving the ester bond between Fmoc₈-Lys₄-Lys₂-Lys- β Ala and Wang resin of Fmoc₈-Lys₄-Lys₂-Lys- β Ala-Wang resin using mixture solvent of TFA (4.75 mL), distilled water (0.125 mL) and TIS (0.125 mL) for 2 h. The reaction solution was filtered through a glass filter frit. The filtrate was precipitated in 10-fold excess cold ether to remove excess reaction reagents, and further washed with ether four times. The product was dried with moderately blowing nitrogen.

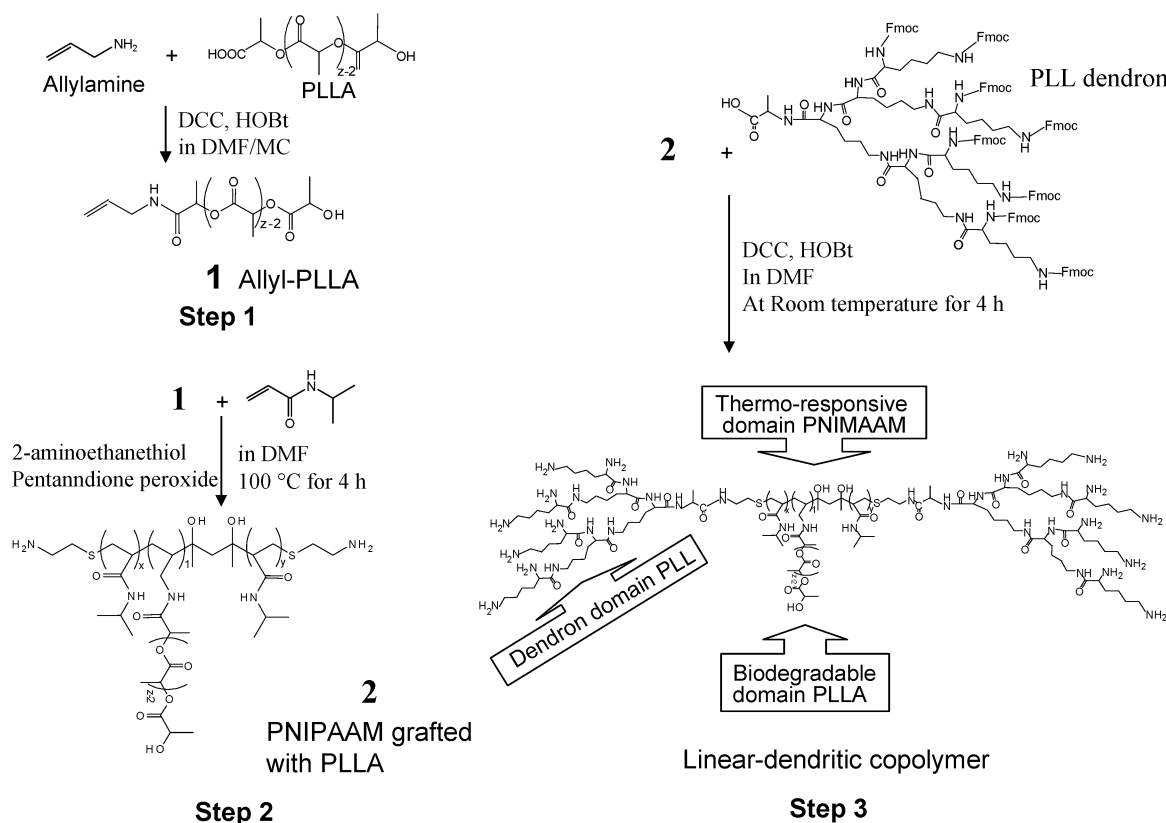
Thermoresponsive-co-biodegradable linear-dendritic copolymer was synthesized by DCC coupling reaction of Fmoc₈-Lys₄-Lys₂-Lys- β Ala (PLL dendron, 80 mg, 0.028 mmol) and PNIPAAm grafted with PLLA (11.25 mg, 0.0035 mmol) in DMF at room temperature for 4 h. The solutions were filtered and precipitated in cold ether. After drying, the linear-dendritic copolymer was dissolved in piperidine (50% in DMF) to cleave off Fmoc groups. After 15 min, the solution was precipitated in cold ether and further washed in ether four times and dried. Final linear-dendritic copolymer was dissolved in water and lyophilized. For further purification, the linear-dendritic copolymer was washed with excess methanol four times to remove unbound PNIPAAm grafted with PLLA and dried with nitrogen blowing. To remove unbound PLL dendron, the linear-dendritic copolymer was dissolved in distilled water at 500 $\text{mg}\cdot\text{mL}^{-1}$. The linear-dendritic copolymer solution was centrifuged at 3000 rpm at 39 °C for 1 h. The supernatant containing unbound PLL dendron was carefully taken out, and fresh distilled water was added for further washing. These purification processes were repeated three times, and the precipitated linear-dendritic copolymer was dissolved in water and lyophilized. The yield of this reaction was 76%.

Chemical and Physical Structures of Linear-Dendritic Copolymer. ¹H NMR. ¹H NMR (Bruker, DRX-400, Billerica, MA) was used to measure the chemical shifts of the products of each synthesis step. For PLLA, PLLA terminated with allyl group and PNIPAAm grafted with PLLA, CDCl_3 was used as a solvent, and the chloroform-*d*₁ resonance was set at 7.27 ppm. For linear-dendritic copolymer, D_2O was used as a solvent, and tetramethylsilane was used as an internal reference. Samples for the ¹H NMR measurements were prepared by dissolving approximately 1 mg each of material in 1 mL of the corresponding solvent.

MALDI-TOF Mass Spectroscopy. MALDI-TOF mass spectra were done on Voyager DE-PRO Biospectrometry Workstation (Perceptive Biosystems). A N_2 laser radiating at 337 nm wavelength with 3 ns pulses was used. Ions generated by the laser pulses were accelerated to 25 kV energy. Distilled water was used as a solvent for linear-dendritic copolymer, PNIPAAm grafted with PLLA and homogeneous PNIPAAm, and THF was used as a solvent for PLLA. Polymer sample solutions at 10 $\text{mg}\cdot\text{mL}^{-1}$ were mixed with a matrix solution of 2,5-dihydroxybenzoic acid (10 $\text{mg}\cdot\text{mL}^{-1}$) at a ratio of 1:9 (v/v, polymer:matrix). The number and weight-average molar masses of the polymers were determined in a linear mode.

Thermoresponsive Properties of Linear-Dendritic Copolymer. UV-Vis Spectroscopy. Transmittance of the linear-dendritic copolymer in PBS (pH 7.4) at 1, 0.5, 0.1, and 0.05 $\text{mg}\cdot\text{mL}^{-1}$ was measured against temperature by UV-vis spectroscopy (PerkinElmer Lambda 25) at 500 nm wavelength. Temperature was increased at rate 1 °C/20 min between 10 and 55 °C. The LCSTs of the linear-dendritic copolymer were defined as temperatures at 95% of maximum transmittance.

Dynamic Light Scattering. The apparent average hydrodynamic radii (R_h) of the linear-dendritic copolymer in PBS (pH = 7.4) at 1, 0.5, and 0.1 $\text{mg}\cdot\text{mL}^{-1}$ were measured as a function of temperature by a dynamic light scattering instrument equipped with an ALV-

Scheme 1. Synthesis of the Thermoresponsive and Biodegradable Linear-Dendritic Copolymer Composed of PNIPAAm, PLLA, and PLL

CGS-8F compact goniometer system, an ALV-5000/EPP multiple τ real time correlator, and an ALV-5000/E/WIN software (ALV, Germany). The light source was a JDS Uniphase helium/neon laser (633 nm, 35 mW, Manteca, CA). Autocorrelation functions of the linear-dendritic copolymer solution at 90° scattering angle were collected three times every half an hour at each temperature between 15 and 45°C , and samples were stabilized for 1 h after each temperature change. The data were fitted using a Cumulants method to derive apparent hydrodynamic radii of the linear-dendritic copolymer. The LCSTs of the linear-dendritic copolymer were defined as the initial break points of R_h -temperature curves.

Biodegradable Properties of Linear-Dendritic Copolymer. Viscometer, MALDI-TOF, and FTIR. The relative viscosity, molar mass, and chemical structure changes of the linear-dendritic copolymer in PBS (pH = 7.4) at $1\text{ mg}\cdot\text{mL}^{-1}$ were measured as a function of time for 35 days by a Cannon-Ubbelohde type viscometer (following the procedures of ASTM D 445 and ISO 3104), MALDI-TOF and FTIR, respectively, at 25 and 37°C . For FTIR measurements, $10\text{ }\mu\text{L}$ linear-dendritic copolymer in PBS (pH = 7.4) solutions at selected degradation time points were applied on a KBr window (KBr DSC UNIPOL, $20\text{ mm} \times 5\text{ mm}$, International crystal labs, Garfield, NJ) and dried at room temperature for 1 day. The IR absorbance of the samples was measured by Thermo Nicolet Avetar 370 FTIR instrument (Madison, WI) at wavelength from 400 to 4000 cm^{-1} .

Particle Size of Linear-Dendritic Copolymer. Transmission Electron Microscopy (TEM). TEM images were acquired on a Philips TEM 400 with an accelerating voltage of 60 kV at a magnification of 50 000 or 100 000 and a slight defocus to enhance contrast. Samples were prepared by dissolving linear-dendritic copolymer in Millipore water ($18\text{ }\Omega$) at $2.5\text{ mg}\cdot\text{mL}^{-1}$, and then $20\text{ }\mu\text{L}$ solution was pipetted onto a holey carbon coated 400 mesh copper grid. The linear-dendritic copolymer solution was allowed to sit for 5 min after excess solution was wicked off to the side with filter paper. Immediately thereafter, $20\text{ }\mu\text{L}$ of 2 wt % phosphotungstic acid solution was pipetted onto the grid. The residual film of liquid was allowed to dry in the air.

Results and Discussion

In the present work, the thermoresponsive-co-biodegradable linear-dendritic copolymer was synthesized by coupling PLL dendron and PNIPAAm grafted with PLLA by the following three steps (Scheme 1). At first, PLLA ($M_w = 2000\text{ g}\cdot\text{mol}^{-1}$) was terminated with allyl group by coupling PLLA with allylamine through DCC reaction with HOBt in DMF/methylene chloride (50:50 v/v) at room temperature. Second, PLLA was grafted to PNIPAAm by free radical polymerization of the PLLA terminated with allylamine macromer and NIPAAm monomer using pentanedione peroxide as an initiator and 2-aminoethanethiol as a transfer agent in DMF under nitrogen condition at 100°C for 4 h. Third, the linear-dendritic copolymer was prepared by DCC coupling reaction of PLL dendrons (Fmoc₈-Lys₄-Lys₂-Lys- β Ala, three generation) and the PNIPAAm grafted with PLLA in DMF at room temperature. The Fmoc group of the linear-dendritic copolymer was cleaved in 30/70 (v/v) mixture of piperidine and DMF, and precipitated in cold diethyl ether. The resulting polymer was purified by using cellulose dialysis membrane (MWCO 3500 Da).

To confirm the success of the syntheses, we characterized the chemical structures of the PLLA, PNIPAAm grafted with PLLA, and linear-dendritic copolymer using ^1H NMR. Figure 1 demonstrated that after allylamine was conjugated with PLLA, the resulting product Ally-PLLA had four new NMR peaks at δ 6.26 (c, $-\text{CH}=\text{CH}_2$), δ 5.80 (d, $-\text{CH}=\text{CH}_2$), δ 3.85 (e, $-\text{NH}-\text{CH}_2-\text{CH}_2-\text{CH}=\text{CH}_2$) and δ 3.46 ppm (f, $-\text{NH}-\text{CH}_2-\text{CH}_2-\text{CH}=\text{CH}_2$) owing to the allylamine component, besides the two characteristic peaks of PLLA at δ 5.15 (a, $-\text{O}(\text{O}=\text{C})-\text{CHCH}_3-$) and δ 1.59 ppm (b, $-\text{O}(\text{O}=\text{C})\text{CHCH}_3\text{O}-$). After Ally-PLLA was grafted to PNIPAAm, the following five new ^1H NMR peaks (Figure 1) occurred due to the incorporation of aminoethanethiol and PNIPAAm: δ 7.93 (g, $-(\text{C}=\text{O})\text{NHCH}-$

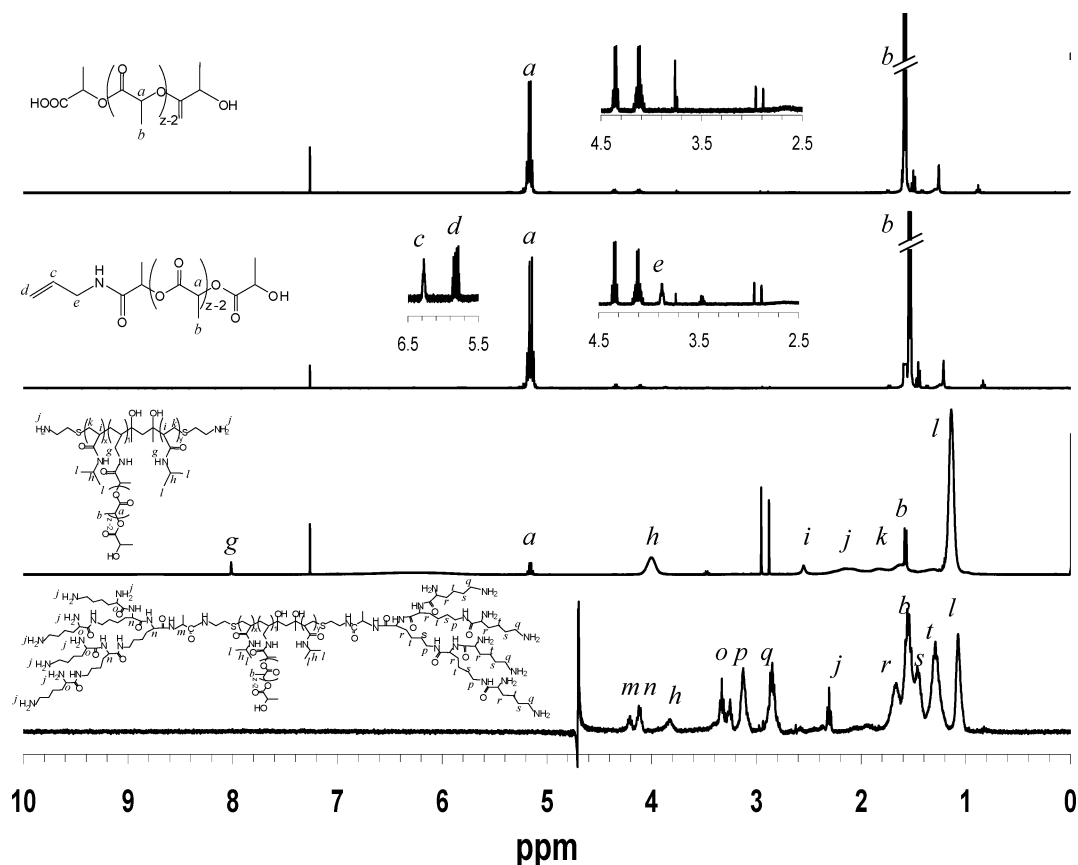


Figure 1. ^1H NMR spectra of PLLA, Allyl-PLLA, PNIPAAm grafted with PLLA and linear-dendritic copolymer.

(CH_3) $_2$), δ 3.97 (h, $-(\text{C}=\text{O})\text{NHCH}(\text{CH}_3)_2$), δ 2.46 (i, $-\text{CH}_2\text{CH}-(\text{C}=\text{O})\text{CH}_2-$), δ 2.07 (j, $-\text{NH}_2$), δ 1.78 (k, $-\text{CH}_2\text{CH}(\text{C}=\text{O})-\text{CH}_2-$), and 1.13 (l: $-(\text{C}=\text{O})\text{NHCH}(\text{CH}_3)_2$) ppm. After PLL dendrons were attached to PNIPAAm grafted with PLLA, the ^1H NMR spectrum of the linear-dendritic copolymer (Figure 1) showed many more peaks in the region of 1 to 4.5 ppm than that of the PNIPAAm grafted with PLLA due to the protons of $-\text{CH}_2-$, $>\text{CH}-$ and $-\text{NH}_2-$ of the PLL dendrons, including δ 4.24 (m, $-(\text{O}=\text{C})\text{CH}(\text{NH}-)\text{CH}_3$, alanine), δ 4.13 (n, $-(\text{O}=\text{C})\text{CHNHCH}_2-$, first and second generation), δ 3.33 (o, $-(\text{O}=\text{C})\text{CHNHCH}_2-$, third generation), δ 3.12 (p, $>\text{CHCH}_2\text{CH}_2-\text{CH}_2\text{CH}_2\text{CH}_2\text{NH}-$), δ 2.84 (q, $>\text{CHCH}_2\text{CH}_2\text{CH}_2\text{CH}_2\text{CH}_2\text{CH}_2\text{NH}_2$), δ 1.65 (r, $>\text{CHCH}_2\text{CH}_2\text{CH}_2\text{CH}_2\text{CH}_2\text{CH}_2\text{NH}-$), δ 1.44 (s, $>\text{CHCH}_2-\text{CH}_2\text{CH}_2\text{CH}_2\text{CH}_2\text{CH}_2\text{NH}-$) and δ 1.28 ppm (t, $>\text{CHCH}_2\text{CH}_2\text{CH}_2-\text{CH}_2\text{CH}_2\text{NH}-$).

To further confirm the success of the linear-dendritic copolymer synthesis, we determined the molar masses and molar mass distributions of the PLLA, PNIPAAm, PNIPAAm grafted with PLLA and linear-dendritic copolymer using MALDI-TOF mass spectroscopy. As shown in Figure 2 and Table 1, the molar masses increased with the steps of the syntheses, in the order of PNIPAAm, PLLA < PNIPAAm grafted with PLLA < linear-dendritic copolymer. The number-average molar mass M_n of the PNIPAAm grafted with PLLA and linear-dendritic copolymer were around 2560 and 4550 $\text{g}\cdot\text{mol}^{-1}$, respectively. The weight-average molar mass of the PNIPAAm grafted with PLLA and linear-dendritic copolymer were around 3280 and 5270 $\text{g}\cdot\text{mol}^{-1}$, respectively. The molar mass distribution of the linear-dendritic copolymer was 1.21 ± 0.13 . Encouragingly, the M_n of the final linear-dendritic copolymer can be theoretically calculated by the sum of 2560 (PNIPAAm-co-PLLA copolymer) and 1936 (two PLL dendrons minus two H_2O), resulting in 4496 (g/mol), which is approximately

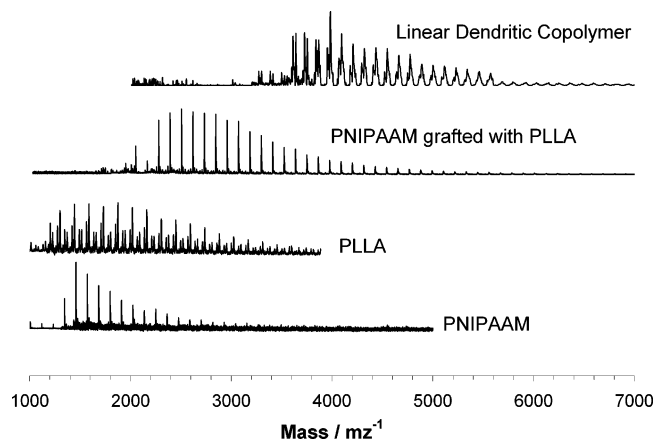


Figure 2. Representative MALDI-TOF spectra of PNIPAAm, PLLA, PNIPAAm grafted with PLLA, and linear-dendritic copolymer.

Table 1. Molar Masses and Molar Mass Distributions of the Polymers

sample id	$M_n/\text{g}\cdot\text{mol}^{-1}$	$M_w/\text{g}\cdot\text{mol}^{-1}$	M_w/M_n
PNIPAAm grafted with PLLA	2560 ± 229	3280 ± 272	1.28 ± 0.12
linear-dendritic copolymer	4550 ± 295	5270 ± 270	1.21 ± 0.13

matching the observed M_n (4550 g/mol) of the final linear-dendritic copolymer. Furthermore, precise measurement of the molecular weight shifts in the individual MALDI-TOF peaks from the PNIPAAm-co-PLLA to the linear-dendritic copolymer confirmed that exact two PLL dendrons were attached on the both ends of the PNIPAAm-co-PLLA.

To characterize the thermoresponsive properties of the synthesized linear-dendritic copolymer, UV-vis spectroscopy was used to study the transmittances of linear-dendritic copolymer in phosphate buffer saline (PBS, pH 7.4) as a

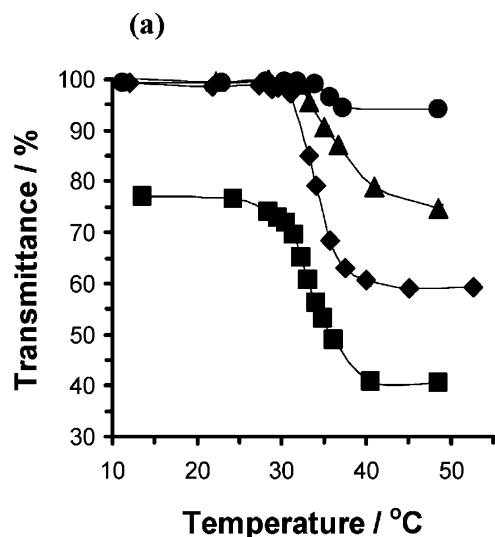


Figure 3. Transmittances of linear-dendritic copolymer, measured by UV-vis spectroscopy, against temperature in PBS (pH 7.4) at concentrations of 0.05 (●), 0.1 (▲), 0.5 (◆), and 1 (■) $\text{mg}\cdot\text{mL}^{-1}$.

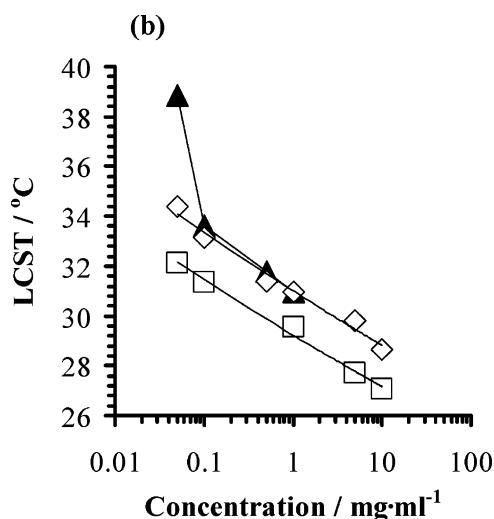


Figure 4. LCSTs of PNIPAAm (◇), PNIPAAm grafted with PLLA (□) and linear-dendritic copolymer (▲) against concentrations in PBS (pH 7.4), measured by UV-vis spectroscopy.

function of temperature with various concentrations (Figure 3). The linear-dendritic copolymer was thermoresponsive, showing LCSTs (defined as temperature at 95% of maximum transmittance) of 31, 32, 34, and 39 °C at concentrations of 1, 0.5, 0.1, and 0.05 $\text{mg}\cdot\text{mL}^{-1}$, respectively, which increased with decreasing the linear-dendritic copolymer concentration. The LCST became obscure with decreasing the concentration of linear-dendritic copolymers. Above the LCST, the transmittance magnitudes decreased with increasing concentration due to the increasing polymer interactions. Figure 4 shows the concentration dependence of the LCSTs of the PNIPAAm, PNIPAAm grafted with PLLA and linear-dendritic copolymer. The LCSTs of PNIPAAm and PNIPAAm grafted with PLLA decreased linearly with logarithmic concentration, and the latter was 2 °C lower than the former due to the hydrophobicity of the PLLA. However, the LCST of the linear-dendritic copolymer showed nonlinear relationship with logarithmic concentration and the highest value compared to that of the other two types of polymers due to the positive charges and hydrophilicity of the PLL.

The thermoresponsive properties of the linear-dendritic copolymer were further confirmed by measuring the hydrody-

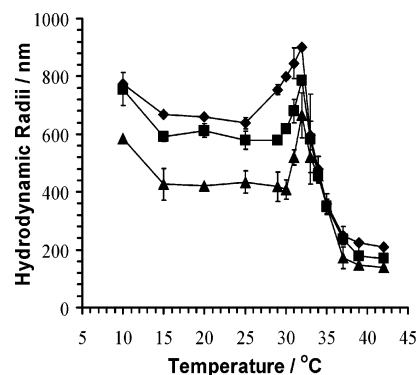


Figure 5. Apparent hydrodynamic radii of linear-dendritic copolymer against temperature in PBS (pH 7.4) at concentrations 0.1 (▲), 0.5 (◆), and 1 (■) $\text{mg}\cdot\text{mL}^{-1}$, measured by dynamic light scattering. Results represented the mean \pm s.d. of three measurements.

amic radii (R_h) of the linear-dendritic copolymer against temperature using dynamic light scattering (Figure 5). The apparent average hydrodynamic radii of the linear-dendritic copolymer in PBS (pH = 7.4) at three concentrations 1, 0.5, and 0.1 $\text{mg}\cdot\text{mL}^{-1}$ showed a temperature dependence in three regions. In the low-temperature ranges of 15–25, 15–29, and 15–30 °C at concentrations 1, 0.5, and 0.1 $\text{mg}\cdot\text{mL}^{-1}$, respectively, R_h was constant. This indicated that the linear-dendritic copolymer was thermally stable in these low-temperature ranges. In the middle temperature ranges starting at 25, 29, and 30 °C at 1, 0.5, and 0.1 $\text{mg}\cdot\text{mL}^{-1}$, respectively, R_h increased with increasing temperature before they reached their respective maximum values at 33 °C. This implied that the linear-dendritic copolymer was not thermally stable and became more and more aggregated due to interchain interactions with increasing temperature in these middle temperature ranges. In both the low and middle temperature ranges, R_h increased with increasing concentrations possibly because interchain interactions increased with increasing concentrations. In the high-temperature ranges, R_h decreased with increasing temperature. Since PLLA with $M_n = 1835 \text{ g}\cdot\text{mol}^{-1}$ was used to synthesize the PNIPAAm grafted with PLLA and the MALDI-TOF results demonstrated that the PNIPAAm grafted with PLLA had $M_n = 2560 \pm 229 \text{ g}\cdot\text{mol}^{-1}$ (Table 1), the average length of the PNIPAAm chain was rather short (DP_n was 5 or smaller). Thus, it is hard to simply explain that the size decrease in the high-temperature range was due to the intrachain interactions of the PNIPAAm component.^{44,45} The possible reasons for the size decrease might be that (1) with increasing temperature, the degradation of the PLLA component became faster so that the aggregates of the linear-dendritic copolymer might be broken down and became smaller and smaller, (2) due to the complexity of the structure of the linear-dendritic copolymer, MALDI-TOF might underestimate the polymers' molar masses,^{46,47} (3) the PLLA component might degrade during the synthesis and purification process, and (4) the final linear-dendritic copolymer might contain impurity like homogeneous PNIPAAm conjugated with PLL dendrons. It is unclear at current stage which one of the above possibilities was dominant. In Figure 5, the LCSTs of the linear-dendritic copolymer, defined as the initial break points of the R_h -temperature curves, were 29 (might be between 25 and 29 °C), 30, and 31 °C at 1, 0.5, and 0.1 $\text{mg}\cdot\text{mL}^{-1}$, respectively. The LCSTs determined by the DLS was slightly lower than those determined by the UV-vis spectroscopy for the same solution concentration, which might be attributed to different instruments for the measurements. Both the DLS and UV-vis results demonstrated that the LCST decreased with increasing concentration. It is worth to mention that the sizes

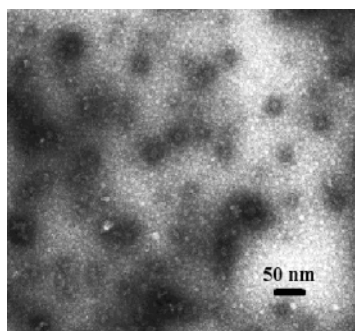


Figure 6. Particle sizes of dendrimer in the dry state, measured by TEM.

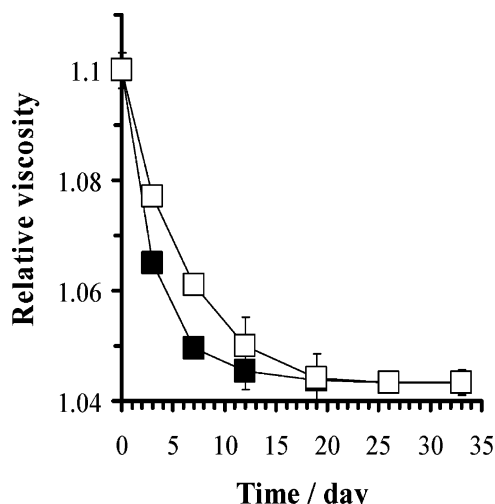


Figure 7. Viscosities of dendrimer against time in PBS (pH 7.4) at 0.1 mg·mL⁻¹ at temperature below (□, 25 °C) and above the LCST (■, 37 °C), measured by Cannon-Ubbelohde type viscometer. Results represented the mean ± s.d. of five measurements.

of the linear–dendritic copolymer in dry state measured by transmission electron microscopy (TEM) were between 20 and 40 nm (Figure 6).

To characterize the hydrolytically degradable properties of the linear–dendritic copolymer, we measured the viscosity and molar mass changes of the linear–dendritic copolymers as a function of time using a Cannon-Ubbelohde viscometer (Figure 7) and MALDI–TOF (Figure 8), respectively, in PBS (pH = 7.4) at temperature below (25 °C) and above the LCST (37 °C). Both the viscosity and molar mass of the linear–dendritic copolymer decreased with time, decreased faster at 37 °C than at 25 °C, and reached a stable value after 19 days. Interestingly, the equilibrium M_n in Figure 8 was around 2727 g·mol⁻¹, and its subtraction from the initial M_n (4220 g·mol⁻¹) was around 1470 g·mol⁻¹, which was close to the M_n (1835 g·mol⁻¹) of the PLLA. The results implied that the linear–dendritic copolymer degraded, and their degradation might be attributed to the hydrolytic degradation of the PLLA component of the linear–dendritic copolymer. To further study the degradation mechanism of the linear–dendritic copolymer, we measured the FTIR spectra of the linear–dendritic copolymer as a function of time (Figure 9(a)). We observed that the peak intensities at ~1760 cm⁻¹ (ester C=O stretching of PLLA), clearly decreased with time and disappeared after 19 days. While the peak intensities at ~1710 cm⁻¹, which was owned to the acid C=O stretching of degraded PLLA increased and overlapped with the peaks at ~1760 and ~1660 cm⁻¹ with time. Since the peaks at ~1660 cm⁻¹, which was attributed to amide C=O stretching of PNIPAAm and PLL, were relatively stable, we used them

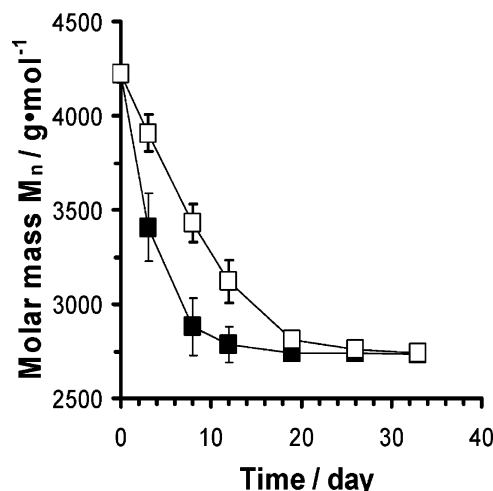


Figure 8. Number molar masses of dendrimer against time in PBS (pH 7.4) at 0.1 mg·mL⁻¹ at temperature below (□, 25 °C) and above the LCST (■, 37 °C), measured by MALDI–TOF. Results represented the mean ± s.d. of five measurements.

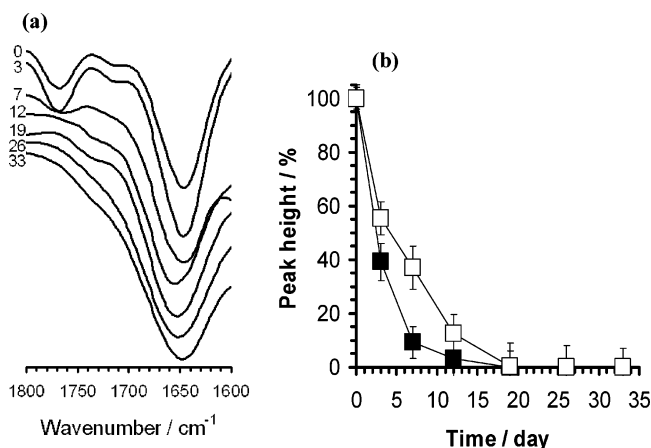


Figure 9. Changes in (a) FTIR spectra; and (b) Relative FTIR peak intensities of dendrimer at ~1760 cm⁻¹ (ester C=O stretching of PLLA) normalized by those at ~1660 cm⁻¹ (amide C=O stretching of PNIPAAm and PLL) at time t to those at initial time. Dendrimer degraded in PBS (pH 7.4) at 0.1 mg·mL⁻¹ with time at temperature below (□, 25 °C) and above the LCST (■, 37 °C). Results represented the mean ± s.d. of five measurements.

as reference peaks to normalize the peak intensities at ~1760 cm⁻¹. The resulted peak height percentage decreased with time and became near 0 after 19 days (Figure 9b). Therefore, the viscosity, MALDI–TOF and FTIR results strongly suggest that the designed linear–dendritic copolymer is biodegradable due to the hydrolytic degradation of the PLLA component. This thermoresponsive and partially degradable copolymer with bulky branched PLL ending groups will have synergistic advantages from each of the three components as described in the Introduction section, and has great potential for thermally targeted and sustained drug delivery across biological barriers in response to temperature and pH changes.

Conclusions

A thermoresponsive-*co*-biodegradable linear–dendritic copolymer was synthesized by DCC coupling reaction of three generation PLL dendron and PNIPAAm grafted with PLLA. ¹H NMR spectra confirmed the chemical structure of the synthesized linear–dendritic copolymer. MALDI–TOF results showed that the linear–dendritic copolymer had number-average and weight molar mass at around 4550 and 5270 g·mol⁻¹, CDV

respectively, and molar mass distribution at 1.21 ± 0.13 . TEM results show that the linear–dendritic copolymer has 20–40 nm diameters in dry state. UV–vis spectroscopy measurements of the transmittance of the linear–dendritic copolymer against temperature demonstrated that the linear–dendritic copolymer was thermoresponsive by showing LCSTs around of 31, 32, 34, and 39 °C at concentrations of 1, 0.5, 0.1, and 0.05 mg·mL⁻¹, respectively, which increased with decreasing the linear–dendritic copolymer concentration. Dynamic light scattering measurements of the hydrodynamic sizes of the linear–dendritic copolymer against temperature further confirmed the thermoresponsive properties of the linear–dendritic copolymer with LCSTs two to three Celsius degree lower than those measured by UV–vis spectroscopy. The linear–dendritic copolymer at 0.1 mg·mL⁻¹ degraded in PBS (pH = 7.4) solutions with both viscosity and molar mass decreasing with time for 19 days due to the hydrolytically degradation of the PLLA component, which was revealed by the FTIR measurements. The linear–dendritic copolymer at 0.1 mg·mL⁻¹ degraded faster at 37 °C than at 25 °C. The thermoresponsive-co-biodegradable linear–dendritic copolymer is currently being developed for targeted and sustained release of therapeutic agents across the blood brain barrier and to the cancerous lesions in response to temperature change.

Acknowledgment. This work was supported by the Special Opportunity Award of the Whitaker Foundation and Penn State Surgery Feasibility Grant. We would like to thank the Mass Spectrometry and Proteomics Core and the Electron Microscopy Core of the Penn State College of Medicine for helping with the MALDI–TOF and TEM experiments, respectively.

References and Notes

- Matthews, O. A.; Shipway, A. N.; Stoddart, J. F. *Prog. Polym. Sci.* **1998**, *23*, 1–56.
- Liu, M. J.; Frechet, J. M. J. *Pharm. Sci. Technol. Today* **1999**, *2*, 393–401.
- Svenson, S.; Tomalia, D. A. *Adv. Drug. Deliver. Rev.* **2005**, *57*, 2106–2129.
- Gitsov, I.; Lin, C. *Curr. Org. Chem.* **2005**, *9*, 1025–1051.
- De Jesus, O. L. P.; Ihre, H. R.; Gagne, L.; Frechet, J. M. J.; Szoka, F. C. *Bioconjugate Chem.* **2002**, *13*, 453–461.
- Tang, M. X.; Redemann, C. T.; Szoka, F. C. *Bioconjugate Chem.* **1996**, *7*, 703–714.
- Choi, J. S.; Joo, D. K.; Kim, C. H.; Kim, K.; Park, J. S. *J. Am. Chem. Soc.* **2000**, *122*, 474–480.
- Choi, Y.; Baker, J. R. *Cell Cycle* **2005**, *4*, 669–671.
- Xiang, J. J.; Tang, J. Q.; Zhu, S. G.; Nie, X. M.; Lu, H. B.; Shen, S. R.; Li, X. L.; Tang, K.; Zhou, M.; Li, G. Y. *J. Gene. Med.* **2003**, *5*, 803–817.
- Haensler, J.; Szoka, F. C. *Bioconjugate Chem.* **1993**, *4*, 372–379.
- Marano, R. J.; Toth, I.; Wimmer, N.; Brankov, M.; Rakoczy, P. E. *Gene Ther.* **2005**, *12*, 1544–1550.
- Marano, R. J.; Wimmer, N.; Kearns, P. S.; Thomas, B. G.; Toth, I.; Brankov, M.; Rakoczy, P. E. *Exp. Eye Res.* **2004**, *79*, 525–535.
- Hussain, M.; Shchepinov, M. S.; Sohail, M.; Benter, I. F.; Hollins, A. J.; Southern, E. M.; Akhtar, S. *J. Controlled Release* **2004**, *99*, 139–155.
- Wu, G.; Barth, R. F.; Yang, W. L.; Chatterjee, M.; Tjarks, W.; Ciesielski, M. J.; Fenstermaker, R. A. *Bioconjugate Chem.* **2004**, *15*, 185–194.
- Backer, M. V.; Gaynutdinov, T. I.; Patel, V.; Bandyopadhyaya, A. K.; Thirumamagal, B. T. S.; Tjarks, W.; Barth, R. F.; Claffey, K.; Backer, J. M. *Mol. Cancer. Ther.* **2005**, *4*, 1423–1429.
- Yang, W. L.; Barth, R. F.; Adams, D. M.; Soloway, A. H. *Cancer Res.* **1997**, *57*, 4333–4339.
- Margerum, L. D.; Campion, B. K.; Koo, M.; Shargill, N.; Lai, J. J.; Marumoto, A.; Sontum, P. C. *J. Alloy. Compd.* **1997**, *249*, 185–190.
- Kobayashi, H.; Kawamoto, S.; Saga, T.; Sato, N.; Hiraga, A.; Ishimori, T.; Konishi, J.; Togashi, K.; Brechbiel, M. W. *Magn. Reson. Med.* **2001**, *46*, 781–788.
- Wiener, E. C.; Brechbiel, M. W.; Brothers, H.; Magin, R. L.; Gansow, O. A.; Tomalia, D. A.; Lauterbur, P. C. *Magn. Reson. Med.* **1994**, *31*, 1–8.
- Konda, S. D.; Wang, S.; Brechbiel, M.; Wiener, E. C. *Invest. Radiol.* **2002**, *37*, 199–204.
- Konda, S. D.; Aref, M.; Wang, S.; Brechbiel, M.; Wiener, E. C. *Magn. Reson. Mater. Phys. Biol. Med.* **2001**, *12*, 104–113.
- Gitsov, I.; Wooley, K. L.; Frechet, J. M. J. *Angew. Chem.-Int. Edit. Engl.* **1992**, *31*, 1200–1202.
- Gitsov, I. In *Advances in Dendritic Macromolecules*; Newkome, G. R., Ed.; Elsevier Science: Amsterdam, 2002; Vol. 5, pp 45–87.
- Gitsov, I.; Ivanova, P. T.; Frechet, J. M. J. *Macromol. Rapid Commun.* **1994**, *15*, 387–393.
- Gillies, E. R.; Frechet, J. M. J. *J. Am. Chem. Soc.* **2002**, *124*, 14137–14146.
- Gitsov, I.; Lambrych, K. R.; Remnant, V. A.; Pracitto, R. J. *Polym. Sci. Pol. Chem.* **2000**, *38*, 2711–2727.
- Jeong, B.; Bae, Y. H.; Lee, D. S.; Kim, S. W. *Nature (London)* **1997**, *388*, 860–862.
- Huang, X.; Lowe, T. L. *Biomacromolecules* **2005**, *6*, 2131–2139.
- Ramkissoon-Ganorkar, C.; Liu, F.; Baudys, M.; Kim, S. W. *J. Controlled Release* **1999**, *59*, 287–298.
- Kurisawa, M.; Matsuo, Y.; Yui, N. *Macromol. Chem. Phys.* **1998**, *199*, 705–709.
- Huang, X.; Nayak, B. R.; Lowe, T. L. *J. Polym. Sci. Pol. Chem.* **2004**, *42*, 5054–5066.
- Turk, M.; Dincer, S.; Yulug, I. S.; Piskin, E. *J. Controlled Release* **2004**, *96*, 325–340.
- Chilkoti, A.; Dreher, M. R.; Meyer, D. E.; Raucher, D. *Adv. Drug. Deliver. Rev.* **2002**, *54*, 613–630.
- Meyer, D. E.; Shin, B. C.; Kong, G. A.; Dewhirst, M. W.; Chilkoti, A. *J. Controlled Release* **2001**, *74*, 213–224.
- Kohori, F.; Sakai, K.; Aoyagi, T.; Yokoyama, M.; Yamato, M.; Sakurai, Y.; Okano, T. *Colloids Surf. B* **1999**, *16*, 195–205.
- Kidchob, T.; Kimura, S.; Imanishi, Y. *J. Chem. Soc. Perk. T. 2* **1997**, 2195–2199.
- Ichikawa, H.; Fukumori, Y. *J. Controlled Release* **2000**, *63*, 107–119.
- Chung, J. E.; Yokoyama, M.; Yamato, M.; Aoyagi, T.; Sakurai, Y.; Okano, T. *J. Controlled Release* **1999**, *62*, 115–127.
- Langer, R. *Acc. Chem. Res.* **2000**, *33*, 94–101.
- Schmidmaier, G.; Wildemann, B.; Stemberger, A.; Haas, N. P.; Raschke, M. *J. Biomed. Mater. Res.* **2001**, *58*, 449–455.
- Cima, L. G.; Vacanti, J. P.; Vacanti, C.; Ingber, D.; Mooney, D.; Langer, R. *J. Biomech. Eng.-Trans. ASME* **1991**, *113*, 143–151.
- Zhang, Z. Y.; Smith, B. D. *Bioconjugate Chem.* **2000**, *11*, 805–814.
- Demina, T.; Grozdova, I.; Krylova, O.; Zhirnov, A.; Istratov, V.; Frey, H.; Kautz, H.; Melik-Nubarov, N. *Biochemistry* **2005**, *44*, 4042–4054.
- Siu, M. H.; He, C.; Wu, C. *Macromolecules* **2003**, *36*, 6588–6592.
- Lowe, T. L.; Benhaddou, M.; Tenhu, H. *J. Polym. Sci., Part B: Polym. Phys.* **1998**, *36*, 2141–2152.
- Montaudo, G.; Samperi, F.; Montaudo, M. S. *Prog. Polym. Sci.* **2006**, *31*, 277–357.
- Schulte, T.; Siegenthaler, K. O.; Luftmann, H.; Letzel, M.; Studer, A. *Macromolecules* **2005**, *38*, 6833–6840.

MA0602730